A&A 530, A56 (2011)
DOI: 10.1051/0004-6361/201116553
© ESO 2011

Astronomy & Astrophysics

Stellar scintillation in the short exposure regime and atmospheric coherence time evaluation

V. Kornilov

Sternberg Astronomical Institute, Universitetskij pr-t, 13, 119992 Moscow, Russia
e-mail: victor@sai.msu.ru

Received 20 January 2011 / Accepted 24 March 2011

ABSTRACT

Aims. Accurately measuring the atmospheric coherence time is still a significant problem despite a variety of applicable methods. The Multi-Aperture Scintillation Sensor (MASS) designed for the vertical profiling of optical turbulence also provides a measurements of coherence time, but its results were found to be biased. Hence there is a need for a more robust method to determine τ_0.
Methods. The effect of smoothing the stellar scintillation by a finite exposure of the detector is considered. The short exposure regime is described and its limits are defined. The re-analysis of previous measurements with the MASS is performed to test the applicability of this approach in real data processing. It is shown that most of the actual measurements satisfy the criteria of short exposures.
Results. The expressions for the mean wind speeds $\bar{V}_2$ in the free atmosphere from the measurement of the scintillation indices are derived for this regime. These values provide an estimate of the atmospheric coherence time τ_0 without the need of empirical calibration. The verification of the method based on real measurements of the resulting τ_0 agree well with independent methods.

Key words. site testing – instrumentation: adaptive optics – atmospheric effects

1. Introduction

In recent decades the adequacy of *optical turbulence* (OT) measurements in the Earth's atmosphere above potential astronomical sites and operating observatories has become more and more important. Developments in astronomy demand more in the way we determine OT. One such requirement is the ability to use cheap tools to monitor the OT automatically and on long time scales.

For these methods, which use modest feeding optics, the analysis of the spatial wavefront distortion is replaced by the analysis of temporal variations of the wavefront inside a limited area. The widely used Differential Image Motion Monitor DIMM (Sarazin & Roddier 1990), which measures the turbulence integrated over the whole atmosphere, and the Multi-Aperture Scintillation Sensor MASS (Kornilov et al. 2003; Tokovinin et al. 2003), which determines the altitude distribution of the OT, belong to these methods.

The transition from a spatial to a spatial-temporal description of the OT is based on the hypothesis of frozen turbulence (Taylor 1938) and was analyzed by many authors (see e.g. Roddier 1981; Martin 1987). A necessary component of this analysis is the knowledge of wind velocities in the atmosphere.

The MASS instrument was developed to measure the vertical distribution of the OT. The MASS data contain information about the temporal properties of stellar scintillation that is necessary to estimate the *atmospheric coherence time* τ_0 with a method that involves the *differential exposure scintillation index* DESI as described in Tokovinin (2002).

After the actual measurements of OT with the MASS, it became clear that the τ_0 values derived in this way were significantly underestimated and therefore required additional calibrations and corrections during analysis (Travouillon et al. 2009). Empirical recipes of correction do not give confidence results because this systematic underestimation may be caused by several factors (Tokovinin 2011). On the other hand, a large and permanently increasing volume of collected data requires uniform treatment for an objective comparison of OT characteristics between various sites.

In this paper we analyze the effect of temporal averaging that affects the scintillation indices measured by the MASS instrument and their role in the evaluation of τ_0. In addition we propose a modification of the DESI method that does not depend on an empirical calibration. The presentation of the modified method is preceded by theoretical description of scintillation in the regime of short exposures.

The regime of short exposures allows us to establish a simple relationship between the measured scintillation statistics and the characteristic wind speed that enters the definition of τ_0. In the last section, the method is tested with MASS data taken at Mt. Shadzhatmaz (Kornilov et al. 2010) and Mt. Maidanak (Kornilov et al. 2009).

We found that the main cause of the mentioned underestimations of τ_0 was the wrong interpretation of the formula for DESI. These discrepancies virtually disappear after the correction in the data processing software.

The modified method does not require any empirical calibration. It is theoretically clearer, and gives an estimate of the mean wind in the free atmosphere as well as a more accurate atmospheric coherence time.

2. Temporal averaging of the scintillation

The theory of weak perturbations implies that the *scintillation index* s^2 – the variance of the relative fluctuations of light intensity – is described by the sum of the scintillation indices

produced by individual turbulent layers:

$$s^2 = \int_0^\infty C_n^2(h)\, W(h)\, \mathrm{d}h, \tag{1}$$

where $W(h)$ is the *weighting function* (WF), which depends on the size and shape of the receiving aperture and does not depend on the altitude distribution of the structural coefficient of the refractive index $C_n^2(h)$. The WF represents a power of the scintillation generated by a layer of unit intensity located at a height h.

The MASS method involves simultaneous measurements of the scintillation indices in four concentric apertures of different diameters (hereafter A, B, C and D), which lead to 10 independent scintillation indices. The vertical OT profile is restored from the measured indices and the theoretically calculated WFs (Tokovinin et al. 2003; Kornilov et al. 2007). The calculation of a set of functions $W(h)$ is based on the assumption that light intensity measurement has a *zero exposure*, i.e. the averaging factor is related only to the receiving aperture.

The scintillation index s^2 measured with finite exposure time is determined by the integrated effect of all turbulent layers along the line of sight as in the case of zero exposure (1) but with another WFs.

The expression for the new WFs $W'(w, \tau, h)$ depends not only on the layer altitude h but also on the wind speed $w = w(h)$ and averaging time τ (Tokovinin 2002; Kornilov 2011). It differs from the expression for $W(h)$ with an additional multiplicand $A_s(w, \tau, f)$ in the integrand:

$$W'(w, \tau, h) = 9.62\lambda^{-2} \int_0^\infty f^{-8/3} \sin^2(\pi r_F^2 f^2)\, A(f)\, A_s(w\tau f)\, \mathrm{d}f. \tag{2}$$

Here, f is the modulus of the spatial frequency, $A(f)$ is spatial aperture filter (axisymmetric for MASS apertures), r_F is the Fresnel radius $r_F^2 = \lambda h$.

Multiplicand $A_s(w\tau f) = A_s(\xi)$ is the spectral filter averaging with the wind shear $w\tau$ and can be expressed through the Bessel functions J_0 and J_1 and Struve functions H_0 and H_1 (Kornilov 2011):

$$A_s(\xi) = 2J_0(2\pi\xi) - \frac{J_1(2\pi\xi)}{\pi\xi} - \pi J_0(2\pi\xi)H_1(2\pi\xi) + \pi J_1(2\pi\xi)H_0(2\pi\xi). \tag{3}$$

It has a simple asymptotic behavior for low values of argument $\xi = w\tau f$: $A_s(\xi) \approx 1 - \pi^2\xi^2/6$, which follows from its series expansion in the neighborhood of 0. The approximation provides an accuracy better than 0.02 until $\pi\xi < 1$. When $\xi \to \infty$, the function $A_s(\xi) \approx 1/\pi\xi$, and starting from $\xi \approx 1$, the relative difference is less than 0.04.

These asymptotes correspond to the two extreme cases: the short and the long exposure regimes. The regime of *short exposures* (SE) considered earlier by Tokovinin (2002) will be the subject of this paper. The regime of *long exposures* (LE) was studied recently by Kornilov (2011) in the application of the potential impact of stellar scintillation on the accuracy of photometric measurements.

The main feature of these regimes is that the weighting function $W'(w, \tau, h)$ can be represented as the product of a function depending on wind shear and the function that independs on winds. It allows one to separate the wind effect and the geometry of light propagation.

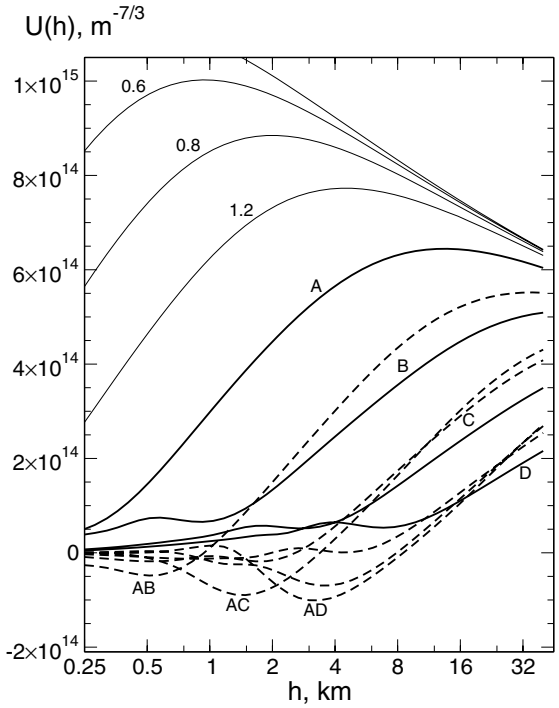

Fig. 1. Weighting functions $U(h)$ for a set of MASS apertures computed for a typical spectral response of its detectors and the light source of spectral class A0 V. The solid curves depict the WFs for normal indices, the dashed curves those for cross-indices. The thin lines denote the functions for a number of smaller apertures, their diameters are marked in centimeters.

3. Short exposures

In Eq. (2) the integrand is significantly different from 0 in the region of intersection of the aperture ($f \lesssim 1/D$) and Fresnel ($f \lesssim 1/r_F$) filters. Outside this domain, i.e. when $f > \min\{1/D, 1/r_F\}$, the integrand rapidly tends to 0. If the wind shear $\tau w \ll \max\{D, r_F\}$ then $f\tau w \lesssim 1$ and hence a quadratic approximation $1 - \pi^2(w\tau f)^2/6$ of the spatial filter $A_s(w, \tau, f)$ can be applied.

Let us replace A_s for a certain aperture with the quadratic approximation in Eq. (2) and take w and τ outside the integral over frequency. Then

$$\begin{aligned} s_\tau^2 &= \int C_n^2(h)\, W'(w, \tau, h)\, \mathrm{d}h \\ &= \int C_n^2(h)\, W(h)\, \mathrm{d}h - \frac{\tau^2}{6} \int C_n^2(h)\, w(h)^2\, U(h)\, \mathrm{d}h. \end{aligned} \tag{4}$$

In this difference the first integral is the scintillation power s_0^2 for zero exposure. The second integral (we denote it as $\mathcal{V}_2^U$) is the atmospheric second moment of wind additionally weighted with $U(h)$. The weighting function $U(h)$ is obtained by multiplying the initial spatial spectrum by $\pi^2 f^2$ and subsequently integrating over f. Because the effect of high-frequency spectral components increases after this multiplication, the functions $U(h)$ become essentially different from those usually used $W(h)$ and have dimensions of $\mathrm{m}^{-7/3}$. The set of $U(h)$ functions is shown in Fig. 1.

Additional features of these WFs are as follows:

– the spectral band width effect is more important than before owing to the high-frequency spectral components, which are more intense. The difference of WFs for white and red stars reaches 10% in aperture A;

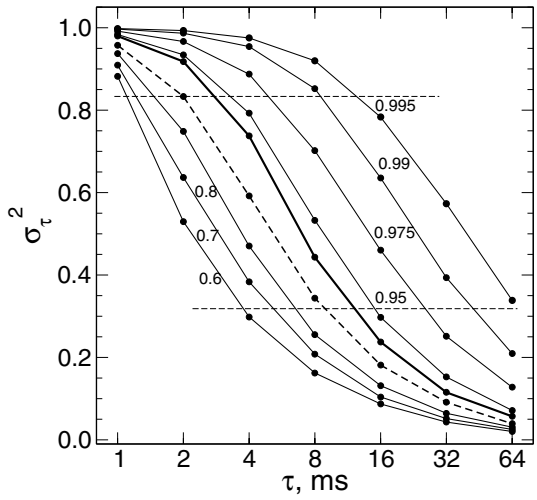

Fig. 2. Indices s^2_τ normalized to s^2_0 as function of an exposure τ. The bold curve corresponds to the median of $\gamma_{12} = 0.938$, the dashed line to the limit of the SE regime $\gamma_{12} = 0.870$. Other curves are marked by appropriate γ_{12}. The upper horizontal line represents the lower boundary of the SE regime, the lower horizontal line the upper limit of the LE regime.

- for an infinitely small aperture an asymptote does not exist because at $D = 0$ the integral diverges. However, there is an envelope of $\sim h^{-1/6}$ to which the curves converge as $D \to 0$ (see Fig. 1);
- the asymptote for the aperture $D \gg r_F$ is also very interesting: $U(h) \approx 17.22\,\lambda^{-2/3}\,D^{-3}\,h^{4/3}$. Compared to the asymptotic behavior of the normal scintillation index, it is chromatic and has a stronger dependence on D.

Note that the WFs shown in the figure by the dashed lines are calculated for cross-indices, i.e. the values obtained directly from the MASS instrument measurements rather than differential indices. Differential indices were always calculated from the normal indices and covariances in the form of linear combinations, but from the viewpoint of the OT restoration it is a superfluous intermediate step, which we have dismissed.

The SE regime and the LE regime are self-reproducible in the sense that if they occur in each turbulent layer they will be observed for the whole atmosphere. To determine the limits of the SE regime, one can use the condition of the applicability of the quadratic approximation of the wind shear filter $A_s(\xi)$, namely that at its border the function is equal to $1-\pi^2\xi^2/6 = 5/6$.

Because for small $w\tau$ this function varies slowly with frequency f within the main spectral peak (its maximum is located at frequency $\lesssim 0.7/r_F$) of the integrand, the value of s^2_τ will also slightly vary with $w\tau$. Consequently we can assume that the quadratic approximation of the form (4) for a given aperture and atmospheric conditions is applicable while $\tau^2\,\mathcal{V}_2^U < s^2_0$ or

$$s^2_\tau > \frac{5}{6}s^2_0. \tag{5}$$

Of course, this inequality defines the SE regime only within some level of accuracy. One should take into account the error of approximation of the function $A_s(\xi)$ ($\approx$0.02) and the contribution of the secondary peaks of the scintillation spectrum. A rough estimate of the accuracy of the numerical factor in (5) is $\approx$0.05.

Similarly, it is possible to write the limit of the LE regime in the form of $s^2_\tau < \frac{1}{\pi}s^2_0$. Both boundaries are indicated in Fig. 2 with dashed lines. The figure demonstrates examples of the typical behavior of the measured indices s^2_τ with exposures ranging from 1 to 64 ms in different wind conditions. Note that the left and right branch of each curve can be generated by different turbulent layers because the contribution of an individual layer is $\sim C_n^2\,w^2$ in the SE regime while it is $\sim C_n^2/w$ in the LE regime.

Table 1. Characteristics of the γ_{21} and γ_{41} distributions for measurements at Mt. Shadzhatmaz in May 2009–June 2010.

Parameter	A	B	C	D	AB
			Distribution of γ_{21}		
Median	0.94	0.95	0.96	0.97	0.95
Out of SE regime, %	18.0	12.5	6.3	3.3	13.8
			Distribution of γ_{41}		
Median	0.77	0.80	0.84	0.87	0.79
Out of SE regime, %	67.0	59.6	49.8	39.6	61.3

4. Verification of the applicability of the SE regime in the MASS measurements

Since the s^2_0 value is calculated and not measured the restriction (5) is not directly applicable. However instead of s^2_0 one can use an additional index measured with a shorter exposure $\tau' < \tau$. Simple algebraic manipulations lead to the condition

$$s^2_\tau > s^2_{\tau'}\frac{5}{6-(\tau'/\tau)^2}. \tag{6}$$

It follows that for exposures $\tau = 2$ ms and $\tau' = 1$ ms s^2_2 should be more than $0.870\,s^2_1$, for 3 and 1 ms $s^2_3 > 0.850\,s^2_1$ and for 4 and 1 ms $s^2_4 > 0.842\,s^2_1$. Condition (6) cannot be used when exposure τ' itself is too long for the SE regime.

The analysis of actual MASS data obtained at Mt. Shatdzhatmaz in the period May 2009 to June 2010 was performed with the usual exposure $\tau = 1$ ms. The special version of the MASS software recorded additional data in output files to later calculate the indices with exposures 2, 4, 8, 16, 32 and 64 ms (see Fig. 2).

Cumulative distributions of ratios $\gamma_{21} = s^2_2/s^2_1$ and $\gamma_{41} = s^2_4/s^2_1$ averaged over a minute are shown in Fig. 3. As might be expected from the form of the WFs (Fig. 1), smaller ratios are observed for smaller apertures, which are more sensitive to the OT motion, and the distribution for the AB cross-index is very close to the curve for the aperture B. Numerical characteristics of the distributions are given in Table 1 and show that the 2-ms measurement is almost always within the SE regime. Only 18% of the measurements in aperture A fail to meet the $\gamma_{21} > 0.870$ condition.

The characteristics of the distributions can vary greatly from season to season. For instance, during the February–March 2010 period, which was characterized by strong winds, the median γ_{21} decreased to 0.90, while the fraction of measurements that do not satisfy the criterion of SE increased to 38%. On the other hand, all measurements fell into the SE regime in October 2009, which was notable for its stable calm weather.

For measurements with 4 ms exposure (value γ_{41}), the situation is radically different. In this case, the vast number of measurements does not satisfy the SE condition and consequently the quadratic approximation can be used only in rare cases and with caution.

A similar analysis was performed for measurements at Mt. Maidanak. The standard MASS data were used, from which

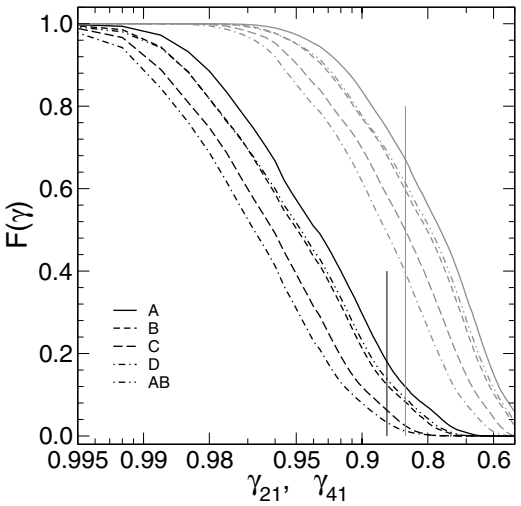

Fig. 3. Cumulative distributions of γ_{21} (black curves) and γ_{41} (gray curves) for the apertures A, B, C, D and AB cross-index based on measurements at Mt. Shatdzhatmaz. Vertical lines cut off the points that do not satisfy the SE regime.

Table 2. Characteristics of the γ_{21} and γ_{31} distributions for measurements at Mt. Maidanak in August 2005–December 2007.

Parameter	A	B	C	D
	Distribution of γ_{21}			
Median	0.92	0.93	0.94	0.96
Out of SE regime, %	19.4	13.3	5.5	0.3
	Distribution of γ_{31}			
Median	0.82	0.84	0.86	0.91
Out of SE regime, %	64.1	57.6	41.5	12.8

indices $s_2^2 = (s_1^2 + \rho_1)/2$ and $s_3^2 = (3s_1^2 + 4\rho_1 + 2\rho_2)/9$ were calculated to construct the cumulative distribution of γ_{21} and $\gamma_{31} = s_3^2/s_1^2$. General properties of these distributions do not differ from those of Mt. Shatdzhatmaz. Some differences are caused by the significantly larger apertures C and D of the first generation device (Kornilov et al. 2003). Characteristics of the distributions are given in Table 2. The fraction of measurements dropping out of SE regime in the A aperture is 19.4% for exposure 2-ms and 64% for 3-ms exposure.

In the situation where γ_{21} approaches unity, a very high precision of the ratio is required because the curves for $\gamma_{21} = 0.995$ and $\gamma_{21} = 0.99$ differ very much. For these curves even 8 ms measurements are in the SE regime.

5. Reduction to zero exposure

Typical exposures of 1 ms are taken with the MASS. This leads to a wind shear on the order of 3 cm assuming a wind speed in the tropopause ~30 m s^{-1}. The value is comparable with the size of the device apertures and with typical Fresnel radius, so a 1 ms exposure cannot be considered to be an infinitely small one. The procedure used to correct indices to zero exposure is provided during the MASS data processing. The algorithm is based on numerical simulations (Tokovinin 2002).

However, for the measurements in the SE regime, the required correction can be calculated with the help of a direct method using the two indices s_1^2 and s_2^2 obtained with different exposures. Although the ratio of exposures may be arbitrary, it is convenient to consider the case of a single τ and a double 2τ exposures. Then the expression (4) becomes

$$s_1^2 = s_0^2 - \frac{\tau^2}{6}\mathcal{V}_2^U, \qquad s_2^2 = s_0^2 - \frac{4\tau^2}{6}\mathcal{V}_2^U. \tag{7}$$

After solving this system for s_0^2, we obtain

$$s_0^2 = \frac{4}{3}s_1^2 - \frac{1}{3}s_2^2. \tag{8}$$

One can express s_2^2 in terms of s_1^2 and covariance ρ_1 of adjacent counts as $2s_2^2 = s_1^2 + \rho_1$. The formula can be re-written as

$$s_0^2 = \frac{7}{6}s_1^2 - \frac{1}{6}\rho_1. \tag{9}$$

The resulting correction is somewhat smaller than the one adopted in Kornilov et al. (2007): $s_0^2 = 1.25s_1^2 - 0.25\rho_1$. Of course, formulas (8) and (9) are exact only if the condition (5) of the SE regime is satisfied for s_2^2.

The statistical error of ρ_1 is very close to that of s_1^2. Consequently, the correction of the scintillation index increases its standard error by a factor of 1.18, which is not significant in practice.

6. Atmospheric second moment of wind

We can estimate the integral $\mathcal{V}_2^U$ from the system of Eqs. (7). Solving the system for the indices measured in the j-aperture ($j = 1, \ldots, 10$) with exposures τ_1 and τ_2 relative to this unknown, we obtain

$$\mathcal{V}_2^{U_j} = \int C_n^2(h)\, w(h)^2\, U_j(h)\, \mathrm{d}h = 6\,\frac{s_{\tau_1}^2 - s_{\tau_2}^2}{\tau_2^2 - \tau_1^2} = \Delta_j, \tag{10}$$

where Δ_j denotes the measured quantity. The integral is of little interest by itself because it includes an additional factor $U_j(h)$, which distorts the contribution of different altitudinal layers. Real estimation of the second atmospheric moment of the wind $\mathcal{V}_2 = \int C_n^2(h)\, w(h)^2\, \mathrm{d}h$ can be obtained if we find a close to unity linear combination $A_U(h)$ of the functions $U_j(h)$.

This type of combination is shown in Fig. 4. Good results can even be obtained when only using functions corresponding to normal indices. The method and results of the decomposition $A_U(h) \approx 1$ are described in detail in Appendix A.

Expansion coefficients of $A_U(h) = \sum_j c_j U_j(h)$ are on the order of 10^{-15} m$^{7/3}$. Summing Eq. (10) for the indices with these coefficients, we obtain

$$\sum_j c_j \Delta_j \approx \mathcal{V}_2. \tag{11}$$

Clearly the boundary layer ($h < 0.5$ km) wind will not be fully accounted for in the integral and the surface wind will be completely excluded despite the strong surface turbulence. The behavior of $A_U(h)$ is similar to the approximating function under the integral defining the intensity of turbulence in the free atmosphere J_{free}. Therefore this quantity can be used for further normalization. The contribution of the surface layer can be accounted for later on base of the DIMM data.

Dividing both sides of the expression (11) by J_{free}, we obtain the mean square of the wind speed $\langle w^2 \rangle$ in the free atmosphere and its expression in terms of measurable quantities:

$$\langle w^2 \rangle = \frac{\mathcal{V}_2}{J_{\mathrm{free}}} = \frac{\sum_j c_j \Delta_j}{J_{\mathrm{free}}}. \tag{12}$$

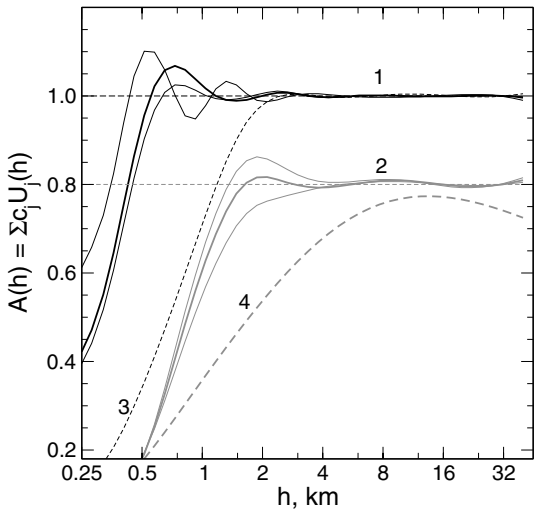

Fig. 4. Approximation $A_U(h)$ of a constant level with help of the set of $U(h)$. Black curves (1) show the approximation with 10 indices, gray (2) with 4 indices. For clarity the gray graphs are shifted to the level of 0.8. Thick lines correspond to the weight of $\sim h$, thin lines to the other power of altitude. Curve 3 corresponds to the weighting of $\sim h^{7/5}$. Gray dashed 4 is the WF for the aperture A.

7. Atmospheric coherence time

It was shown by Kellerer & Tokovinin (2007) that the mean wind $\bar{V}_2$ can be a good estimator of $\bar{V}_{5/3}$, which is used in the definition of the atmospheric coherence time τ_0. We recall that the instrument FADE (Fast Defocusing of stellar image, Tokovinin et al. 2008) measures the time constant (interferometric coherence time) also using $\bar{V}_2$. Although the authors indicate that on average $\bar{V}_2 \approx 1.1\bar{V}_{5/3}$, we will assume that both values are equivalent in the following argumentation.

Evaluation of $\bar{V}_2$ (in the free atmosphere) from the measurements is obtained directly from the formula for $\langle w^2\rangle$:

$$\bar{V}_2 = \langle w^2\rangle^{1/2} = \frac{(\sum_j c_j\Delta_j)^{1/2}}{J_{\rm free}^{1/2}}. \quad (13)$$

Substituting this value in the definition of the atmospheric time constant τ_0, we obtain the following expression:

$$\tau_0 = 0.314\frac{r_0}{\bar{V}_2} = 0.058\lambda^{6/5}J_{\rm tot}^{-3/5}\frac{J_{\rm free}^{1/2}}{(\sum_j c_j\Delta_j)^{1/2}}, \quad (14)$$

where we substituted the Fried parameter r_0 with OT intensity $J_{\rm tot}$ in the whole atmosphere. For the wavelength $\lambda = 500$ nm:

$$\tau_0 = 1.593\times10^{-9}J_{\rm tot}^{-3/5}\frac{J_{\rm free}^{1/2}}{(\sum_j c_j\Delta_j)^{1/2}}. \quad (15)$$

If there is information about the OT power in the boundary layer and surface wind speed V_0, its contribution can be accounted for at the stage of calculating the mean wind $\bar{V}_2$. In order to do this, we correct the mean square of the wind speed by adding V_0^2 in proportion of the surface layer intensity $J_{\rm GL}$:

$$\langle\tilde{w^2}\rangle = \frac{\langle w^2\rangle J_{\rm free} + V_0^2 J_{\rm GL}}{J_{\rm tot}}, \quad (16)$$

or

$$\bar{V}_2 = \frac{\left(\sum_j c_j\Delta_j + V_0^2 J_{\rm GL}\right)^{1/2}}{J_{\rm tot}^{1/2}}. \quad (17)$$

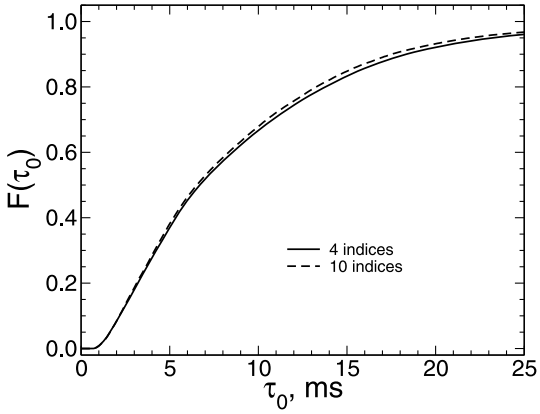

Fig. 5. Cumulative distribution of free atmosphere τ_0 from measurements at Mt. Shatdzhatmaz obtained using $s_1^2 - s_2^2$ differences with decomposition in 4 (solid line) and 10 (dashed line) indices.

Substituting the corrected value in formula (15), we obtain an estimation of the atmospheric coherence time for the whole atmosphere:

$$\tau_0 = 1.593\times10^{-9}\frac{J_{\rm tot}^{-1/10}}{(\sum_j c_j\Delta_j + V_0^2 J_{\rm GL})^{1/2}}. \quad (18)$$

Note that the usual method of adding coherence time $\tau_0^{-5/3} = \tau_{\rm GL}^{-5/3} + \tau_{\rm free}^{-5/3}$ is not correct if used to calculate $\bar{V}_2$, which has square metric.

The relative accuracy of τ_0 does not practically depend on the accuracy of the $J_{\rm tot}$, and is twice as good as the accuracy of the measured Δ_j.

8. Verification of the method of evaluation τ_0

The method presented here was tested with data obtained at Mt. Shadzhatmaz and Mt. Maidanak, which were analyzed in Sect. 4. To construct $\sum_j c_j\Delta_j$, we used the coefficients from the Table A.1 defined for stars of spectral class A0 V. This simplification introduces a systematic error when processing the measurements of stars of other spectral classes, which is why further results should not be regarded as final (less than 5%, see Sect. 3). We also computed the coherence time for free atmosphere, i.e. the $J_{\rm free}$ value was used instead of $J_{\rm tot}$ in formula (15).

For the measurements at Mt. Shadzhatmaz, the differences Δ_j were computed from indices s_1^2 and s_2^2. The results of the evaluation are shown in Fig. 5, where the cumulative distributions of τ_0 obtained with different decompositions are presented. The method results in 6.69 ms median when using 4 normal indices and 6.53 ms using all 10 indices. The difference between these distributions is completely explained by the fact that usage of all indices involves an additional contribution of moving turbulence between 0.5 and 1 km.

For the standard MASS output (Maidanak campaign), the normal indices s_1^2, s_2^2, and s_3^2 were used to study biasing of τ_0 estimations with a different temporal span. At first we investigated the effect of the DESI formula correction, i.e. a replacement of the index s_0^2 with the index s_1^2. As can be seen from Fig. 6, the correction increases the τ_0 estimations by a factor $\approx$1.4. The cumulative distributions of the coherence time calculated from $s_1^2 - s_2^2$ and $s_1^2 - s_3^2$ are also presented in the figure. Evidently that the median differs only slightly for the corrected DESI algorithm (5.82 ms) and the 2 ms median (5.98 ms).

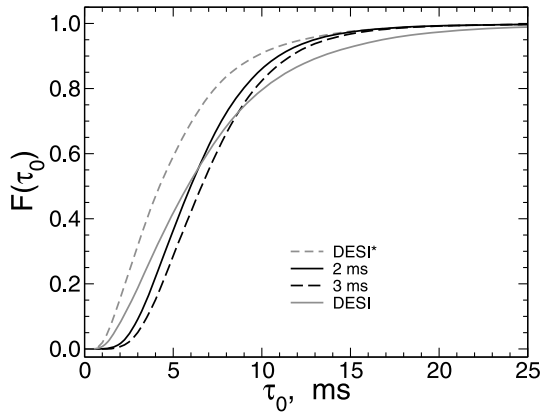

Fig. 6. Cumulative distribution of free atmosphere τ_0 from measurements at Mt. Maidanak obtained using DESI (grey dashed – before software correction, grey solid – after) and using $s_1^2 - s_2^2$ and $s_1^2 - s_3^2$ differences (black solid and dashed curves respectively).

The τ_0 values obtained with s_3^2 are systematically higher by ≈0.6 ms than τ_0 calculated with s_2^2. This shift is caused by the 3 ms exposure beyond the SE regime. When the τ_0 increases, the greater number of the 3 ms measurements satisfies the criterion of SE and because of that, the relative difference between the curves for 2 ms and 3 ms is reduced, becoming less than 4% at $\tau_0 \approx 15$ ms. To obtain the systematic shift of the 2 ms curve, additional measurements with a shorter exposure are required. However, taking into account the quadratic dependence of indices on exposure, we can estimate that its median is not overstated by more than 5%.

Random errors of τ_0 were computed during the averaging of $\bar{V}_2$ over 1 min as the standard error of the mean. The relative error of $\bar{V}_2$ is approximately constant in the entire range of values. At very low winds (less than 5 m s^{-1}) the errors increase. The median of the relative error is ≈0.02, only 1% of the measurements have errors greater than 0.1.

9. Discussion and conclusion

The analysis of actual MASS measurements described in Sect. 4 has shown that for the commonly used 1 ms exposure, 80% of the cases are within the SE regime and that the correction to zero exposure (9) is suitable. Despite some conventionality of the regime boundary definition, it cannot be significantly weakened. On the contrary, the study of real data requires some tightening of the limit to guarantee that all turbulent layers are within the SE regime. Our statistics shows that exposures of 3 ms rarely satisfy the criterion of SE.

Such a control is important because measurements of τ_0 in large wind shear will be affected by systematic errors. Fortunately these cases are not as interesting as the opposite ones.

The reaction of the DESI method on fast turbulence motion is not so evident. One can derive from the definition of the differential exposure signal (Tokovinin 2011) and formula (10):

$$\mathrm{DESI} = \frac{2}{9}(3s_1^2 - 4\rho_1 + \rho_2) = \frac{3}{4}(\Delta_A^{12} - \Delta_A^{13}). \quad (19)$$

This means that the DESI method estimates the coherence time not by using the atmospheric wind moment, but its derivative with exposure. The DESI differences are smaller by an order of magnitude than the values themselves and therefore the DESI method is noisier. Indeed, for Mt. Maidanak data the median of relative random errors is ≈0.03 using the difference $s_1^2 - s_2^2$, while using DESI the median of relative errors amounts ≈0.1.

The case of a calm atmosphere is most interesting from the viewpoint of adaptive optics and interferometry. In this situation the differences of the indices are small and poorly defined owing to an increase of the relative error. The most dangerous is a systematic error due to an incorrect accounting for photon noise. To reduce the impact of these errors, an adaptable choice of exposure may be realized (Tokovinin 2011).

Fortunately, in real situations this effect is not too large. For example, measurements at Mt. Maidanak show that an error $\Delta p = 0.01$ in the parameter p for photon noise correction changes the τ_0 median by 0.05 ms. At $\tau_0 \approx 15$ ms (95% level of cumulative distribution) this error results in a shift of the curve by 0.7 ms when used $s_1^2 - s_2^2$ and 0.3 ms when $s_1^2 - s_3^2$.

Generally speaking, the SE regime is not very suitable to determine wind conditions. Much more accurate results can be obtained by the determination of the averaging time t for which the index s_t^2 becomes equal to $s_0^2/2$. This method is similar to the calculation of correlation peak width, see e.g., Caccia et al. (1987). However, in the middle domain (see Fig. 2) the behavior of s_t^2 indicates that similar integral characteristics are closer to the mean wind speed $\langle w \rangle$ than to the mean square $\langle w^2 \rangle$. The mean speed may be used for some applications, but for the τ_0 evaluation the value $\langle w^2 \rangle$ is more suitable.

The analyzed data were obtained at sites with rare high-altitude jet streams. For other observatories, especially those closer to the equator, the situation could be worse. There it will make sense to reduce the exposure to 0.5–0.7 ms, which is equivalent to increasing the wind range by 1.5–2 times. The main objective of a correct choice of exposure is to ensure that we are within the SE regime for a statistically overwhelming fraction of cases.

The main advantage of making measurements in the SE regime is the simplicity of the theoretical description and its practical usage. The described method for a τ_0 evaluation does not contain any empirical calibration, it gives more accurate estimations and additional information about the mean wind in the free atmosphere.

All quantities on the right hand side of Eq. (15) are measured with MASS/DIMM simultaneously. However, the joint MASS/DIMM data processing was realized only in the recent version of the program *atmos* (Kornilov et al. 2010) and the algorithm described in Sect. 7 will be implemented in the next release of this version. An alternative way is to use a fairly simple post-processing of existing MASS output, but in both cases the meteo data on the surface wind are additionally needed to take the ground layer into account. Free atmosphere τ_0 evaluation using both methods is implemented starting with the *atmos-2.97.3* version.

Acknowledgements. The author thanks his colleagues who took part in campaigns of optical turbulence measurements at Mt. Maidanak and Mt. Shatdzhatmaz, by whose efforts the data set used in the analysis was collected. Concerned discussion on the atmospheric coherence time from MASS data with participants of the conference "Comprehensive characterization of astronomical sites" also stimulated the implementation of this work. The author is particularly grateful to A. Tokovinin and N. Shatsky for useful discussions, T. Travouillon for his efforts to make the paper clearer and M. Sarazin for his interest in the appearance of this work.

Table A.1. Coefficients c_j (10^{-15} m$^{7/3}$) of the h^0 decomposition in WFs $U(h)$ when we used all indices, 4 normal indices, 4 normal indices for the original MASS device – Cols. 2, 3, 4 respectively.

Aperture	c_j	c_j	c_j
A	3.229	2.981	2.504
B	3.191	−3.641	−2.823
C	0.080	2.880	2.960
D	−0.826	0.273	−0.730
AB	−5.040	...	...
AC	1.124	...	...
AD	0.013	...	...
BC	−0.810	...	...
BD	0.547	...	...
CD	0.166	...	...
Noise Factor	4.16	2.21	2.54

Appendix A: Decomposition in the weighting functions

The decomposition of the atmospheric wind moment $\mathcal{V}^2$ is done in the same way as an expansion of altitude atmospheric moments with sets of measured indices (Tokovinin et al. 2003) in the program *atmos*. In this case we solve the system of linear equations $\boldsymbol{Uc} = \mathbf{1}$, where $\boldsymbol{U}$ is the WFs matrix with the dimension $k \times n$, $\boldsymbol{c}$ is the vector of coefficients, $\mathbf{1}$ is the unit vector corresponding to the altitude grid $\boldsymbol{h}$. The number of nodes $n = 50$ is significantly greater than the maximal number of indices $k = 10$. As usual a log-uniform grid is used, which has more nodes at low altitudes.

The system is solved by SVD with a regularization of the solution by discarding low singular values $s_i < 10^{-3}\, s_0$. The quality of the solution was controlled by two parameters: the maximum deviation from 1 (not accounting for the initial part of the curve) and the noise enhancement factor $NF = (\sum_j c_j^2)^{1/2} / \sum_j c_j$. The solution depends on how the system was weighted. We used an implicit weight by grid density and some explicit weight.

Without the explicit weight, the solution has the first maximum at the minimum altitude but strongly oscillates and has large $NF > 20$. The study of additional weight in the form of $\sim h^p$ has shown that if $p \approx 1$ the solution is good enough: it is close to 1 and has a moderate NF value.

The approximating curves $A_U(h)$ calculated with all 10 indices and only 4 normal indices are shown in Fig. 4. The curve for aperture A, for which an index and temporal covariances are used in the DESI method to assess the atmospheric coherence time, is also shown. The coefficients c_j are presented in Table A.1 for all variants. They were calculated for a typical set of MASS apertures, its detector response and A0 V spectral class of light source.

The approximation that uses all indices is close to 1 for all nodes of the typical grid for restoration of the OT profile. There is a slight (≈0.06) excess at the altitude of 0.7 km and the difference for other nodes is lower. The approximation with only 4 normal index looses 25% of the contribution of 1 km layer and almost 75% of the contribution of 0.5 km layer. It is expected that the decomposition in the complete set of indices will give an estimation of τ_0 with smaller systematic errors because the noise properties of cross-indices are not worse than those of normal indices and the factor NF in the first variant is only twice as large.

References

Caccia, J. L., Azouit, M., & Vernin, J. 1987, Appl. Opt., 26, 1288
Kellerer, A., & Tokovinin, A. 2007, A&A, 461, 775
Kornilov, V. G. 2011, Astron. Lett., 37, 40
Kornilov, V., Tokovinin, A. A., Vozyakova, O., et al. 2003, in SPIE Conf. Ser. 4839, ed. P. L. Wizinowich, & D. Bonaccini, 837
Kornilov, V., Tokovinin, A., Shatsky, N., et al. 2007, MNRAS, 382, 1268
Kornilov, V., Ilyasov, S., Vozyakova, O., et al. 2009, Astron. Lett., 35, 547
Kornilov, V., Shatsky, N., Voziakova, O., et al. 2010, MNRAS, 408, 1233
Martin, H. M. 1987, PASP, 99, 1360
Roddier, F. 1981, Prog. Opt., 19, 281
Sarazin, M., & Roddier, F. 1990, A&A, 227, 294
Taylor, G. I. 1938, Roy. Soc. London Proc. Ser. A, 164, 476
Tokovinin, A. 2002, Appl. Opt., 41, 957
Tokovinin, A. 2011 [arXiv:1101.3211]
Tokovinin, A., Kornilov, V., Shatsky, N., & Voziakova, O. 2003, MNRAS, 343, 891
Tokovinin, A., Kellerer, A., & Coudé du Foresto, V. 2008, A&A, 477, 671
Travouillon, T., Els, S., Riddle, R. L., Schöck, M., & Skidmore, W. 2009, PASP, 121, 787